Mobile Robots - Current Trends, Chapter 13: Epi.q Robots

MOBILE ROBOTS

CURRENT TRENDS

Edited by **Zoran Gacovski**

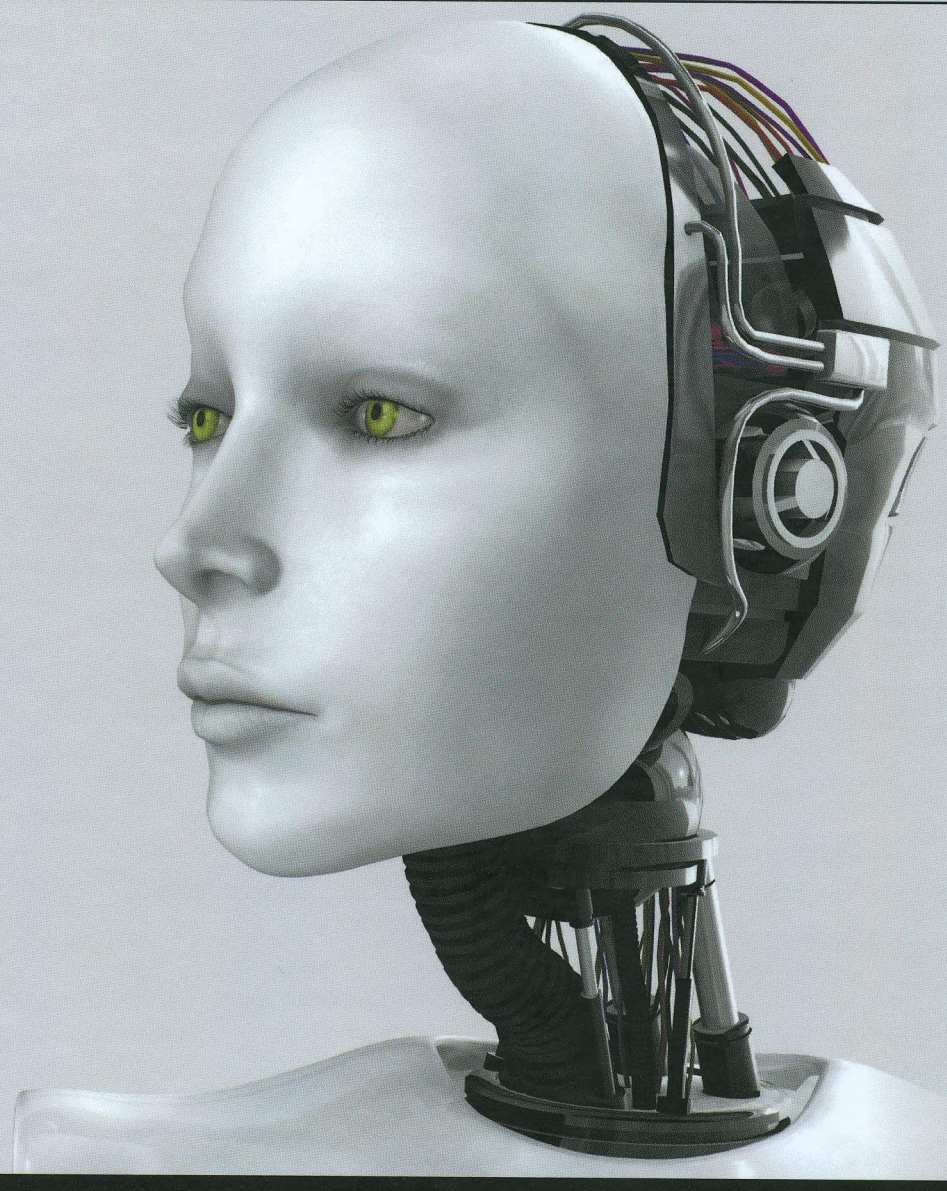

INTECH

MOBILE ROBOTS – CURRENT TRENDS

Edited by **Zoran Gacovski**

INTECHWEB.ORG

Mobile Robots – Current Trends
Edited by Zoran Gacovski

Published by InTech
Janeza Trdine 9, 51000 Rijeka, Croatia

Publishing Process Manager Bojana Zelenika
Technical Editor Teodora Smiljanic
Cover Designer Jan Hyrat
Image Copyright Sarah Holmlund, 2011. Used under license from Shutterstock.com

First published September, 2011
Printed in Croatia

A free online edition of this book is available at www.intechopen.com
Additional hard copies can be obtained from orders@intechweb.org

Mobile Robots – Current Trends, Edited by Zoran Gacovski
p. cm.
ISBN 978-953-307-716-1

Contents

13

Epi.q Robots

Giuseppe Quaglia[1], Riccardo Oderio[1], Luca Bruzzone[2]
and Roberto Razzoli[2]
[1]*Politecnico di Torino*
[2]*University of Genova*
Italy

1. Introduction

Over the last few years there have been great developments and improvements in the mobile robotics field, oriented to replace human operators especially in dangerous tasks, such as mine-sweeping operations, rescuing after earthquakes or other catastrophic events, fire-fighting operations, working inside nuclear power stations and exploration of unknown environments.
Different locomotion systems have been developed to enable robots to move flexibly and reliably across various ground surfaces. Usually, mobile robots are wheeled, tracked and legged ones, even if there are also robots that swim, jump, slither and so on. *Wheeled robots* are robots that use wheels for moving; they can move fast with low energy consumption, have few degrees of freedom and are easy to control, but they cannot climb great obstacles (in comparison with robot dimensions) and can lose grip on uneven terrain. *Tracked robots* are robots that use tracks for moving; they are easily controllable, also on uneven terrain, but are slower than wheeled ones and have higher energy consumption. *Legged robots* are robots that use legs for moving; they possess great mobility and this makes them suitable for applications on uneven terrain; conversely, they are relatively slow, require much energy and their structure needs several actuators, with increased control complexity. Of course each robot class has advantages and drawbacks, thus scientists designed new robots, trying to comprise the advantages of different robot classes and, at the same time, to reduce the disadvantages: these robots are called *Hybrid robots*.

1.1 Background

Literature presents numerous interesting solutions for robots moving in structured and unstructured environments: some of them are here presented. The Spacecat, Whegs and MSRox can be considered smart reference prototypes for this work; the others are interesting solutions that, using different mechanisms, accomplish similar tasks.
Spacecat (Siegwart et al., 1998) is a smart rover developed at the École Polytechnique Fédérale de Lausanne (EPFL) by a team leaded by prof. Roland Siegwart, in collaboration with Mecanex S.A. and ESA. The locomotion concept is a hybrid approach called *Stepping triple wheels*, that shares features with both wheeled and legged locomotion. Two independently driven sets of three wheels are supported by two frames. The frames can rotate independently around the main body (payload frame) and allow the rover to actively lift one wheel to step climb the obstacle. Eight motors drive each wheel and frame independently. During climbing

operation, the center of gravity of the rover is moved outside the contact surface formed by the four wheels. Thus the rover gets out of balance and falls with its upper wheel onto the obstacle; nevertheless no displacement of the center of gravity is required when the rover moves over a small rock; therefore, small object can be passed without any special control commands.

Whegs and Mini-Whegs (Allen et al., 2003; Quinn et al., 2003; Schroer et al., 2004) are hybrid mobile robots developed at the Center for Biologically Inspired Robotics Research at Case Western Reserve University, Cleveland, Ohio. The *Whegs* were designed using abstracted principles of cockroach locomotion. A cockroach has six legs, which support and move its body. It typically walks and runs in a tripod gait where the front and rear legs on one side of the body move in phase with the middle leg on the other side. The front legs swing head-high during normal walking so that many obstacles can be surmounted without significant gait changes. These robots are characterized by three-spoke locomotion units; they move faster than legged vehicles and climb higher barriers than wheeled ones of similar size. A single propulsion motor drives both front and rear axles and a servo actuated system controls the steering, similarly to automobile vehicle. With regard to Whegs locomotion: while the robot is walking on flat ground, three of the wheel-legs are 60° out of phase with the other three wheel-legs, which allows the robot to use an alternating tripod gait. This gait requires that the two front wheel-legs be out of phase with each other. When an obstacle is encountered, passive mechanical compliance allows the front legs to come back into phase with each other, so that they can both be used to pull the robot up and over the obstacle. After the robot has pulled itself over the obstacle, the front legs fall back into the previous pattern, thus the robot returns to an alternating tripod gait. *Whegs II*, the next generation of Whegs vehicles, incorporates a body flexion joint in addition to all of the mechanisms that were implemented in Whegs I. This actively controlled joint allows the robot to change its posture in a way similar to the cockroach, thus enabling it to climb even higher obstacles. The active body joint also allows the robot to reach its front legs down to contact the substrate during a climb and to avoid the instability of high-centering. Its aluminum frame and new leg design contributed in making Whegs II more robust than Whegs I. *Whegs VP* is a hybrid of the Whegs I and II vehicles. It is most similar in design to Whegs II, but lacks the body flexion joint. It combines the simplicity and agility of Whegs I with the durability and robustness of Whegs II. Improved legs and gait adaptation devices were implemented in its design. The *Mini-Whegs* are highly mobile, robust, and power-autonomous vehicles employ the same abstracted principles as Whegs, but on a scale more similar to the cockroach and using only four locomotion units. These robots, 90 mm long, can run at sustained speeds of over 10 body lengths per second and climb obstacles higher than the length of their legs. One version, called Jumping Mini-Whegs, has also a self-resetting jump mechanism that enables it to surmount obstacles as high as 220 mm, such as a stair.

MSRox (Dalvand & Moghadam, 2006) is an hybrid mobile robot developed by prof. Moghaddam and Dalvand at Tarbiat Modares University, Tehran, Iran. The MSRox employs an hybrid driving unit called *Star-Wheel*, designed for traversing stairs and obstacles. It is a three-legged wheel unit having three radially located wheels, mounted at the end of each spoke. Each Star-Wheel has two rotary axes: one for the rotation of the wheels, when MSRox moves on flat surfaces or passes over uphill, downhill, and slope surfaces; the other for the rotation of the Star-Wheel, when MSRox climbs or descends stairs and traverses obstacles. The four locomotion units are assembled on a central body. The robot can advance on ground, when only the wheel rotation is driven, or climb over an obstacle, when only the locomotion

unit is driven. The presented version of MSRox has only two motors: one motor controls the rotation of the 12 wheels while the other controls the rotation of the Star-Wheels; the steering function is not implemented.
RHex (Saranli et al., 2001; 2004), developed first at the McGill University and University of Michigan and then at the Carnegie Mellon Robotics Institute, is characterized by compliant leg elements that provide dynamically adaptable legs and a mechanically self-stabilized gait. This hexapod robot, cockroach-inspired, uses a simple mechanical design with one actuator per leg and it is capable of doing a wide variety of tasks, such as walking, running, leaping over obstacles and climbing stairs.
Hylos (Grand et al., 2004), developed at the Université Pierre et Marie Curie, is characterized by a wheel-legged locomotion unit. Legs and wheels are independently actuated, therefore it uses wheels for propulsion and internal articulation to adapt its posture. It is a lightweight mini-robot with 16 actively actuated degrees of freedom.
VIPeR (Galileo Mobility Instruments & Elbit Systems Ltd, 2009), codeveloped by Elbit System and Galileo Mobility Instruments, is characterized by the *Galileo Wheel*, a patented system developed by Galileo Mobility Instruments ltd. The Galileo Wheel combines wheel and track in a single component, switching back and forth between the two modes within seconds. This technology enables the device to use wheels whenever possible, and tracks whenever needed.
Lego Mindstorm Artic Snow Cat (Lego Mindstorm, 2007) is characterized by four sets of triangular tracked treads that can rotate in two ways. In standard drive the treads move like a tank. When the going gets tough it can turn all four treads on the center axis, or to go through deep water it can run on the ends of its triangular treads for extra lift.
Packbot (iRobot, 2010; Mourikis et al., 2007), developed by iRobot, is a tracked vehicle with *flippers*. The flippers enable the robot to climb over obstacles, self right itself and climb stairs, enhancing ability over a simple tracked robot.
Scout II (Poulakakis et al., 2006; 2005) is characterized by a fast and stable quadrupedal locomotion. It consists of a rigid body with four compliant rigid prismatic legs. One single actuator per leg, located at the hip, allows active rotation of the leg. Each leg assembly consists of a lower and an upper part, connected via springs to form a compliant prismatic joint.

2. Mechanical architecture

Epi.q robots can be classified as hybrid robots, since their locomotion system shares features with both wheeled and legged robots. They are smart mini robots able to move in structured and unstructured environments, to climb over obstacles and to go up and down stairs. The robots do not need to actively sense obstacles for climbing them, they simply move forward and let their locomotion passively adapt to ground conditions and change accordingly without active control intervention: from rolling on wheels to stepping on rotating legs and vice-versa. Using wheels whenever possible and legs only when needed, their energy demand is really low in comparison with tracked and legged robots having similar obstacle crossing capability.

2.1 Chassis

Epi.q mechanical architecture consists of: a forecarriage, a central body and a rear axle, as shown in Figure 1. The forecarriage is composed of a frame linked to two driving units, that generate robot traction. The forecarriage frame houses motors and electronics, protecting them from dust and from potentially dangerous impacts against obstacles. The driving units are three-legged wheel units having attached thereto three wheels; they house the

transmission system and therefore they control robot locomotion. The rear axle comprises two idle wheel units, consisting of an idle three-legged wheel unit with three radially located idle wheels, mounted at the end of each spoke. The central body is a platform which connects forecarriage and rear axle, where a payload can be placed.
Two passive revolute joints, mutually perpendicular, link front and rear part of the robot,

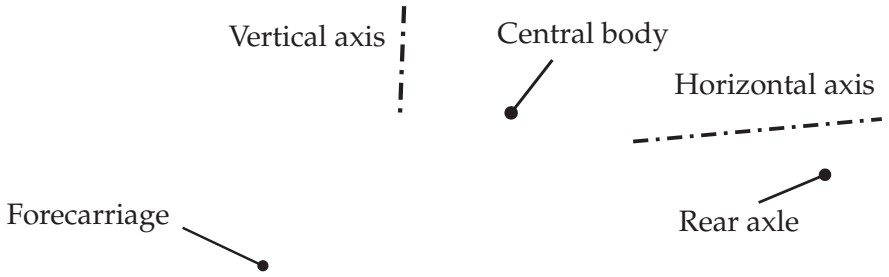

Fig. 1. Epi.q mechanical architecture

as shown in Figure 1. The vertical joint allows robot steering, while the horizontal joint guarantees a correct contact between wheels and ground, also in presence of uneven terrain.The angular excursion of the vertical and horizontal joints is limited by means of suitable mechanical stops.
Epi.q robots implement a differential steering, that provides both driving and steering functions. Differently choosing driving unit speeds, differently the instantaneous center of rotation is positioned along the common driving unit axis, so that an angle between front and rear part is generated by kinematic conditions and the robot can follow a specific path. Basically, a differential steering vehicle consists of two wheels mounted onto a device along the same axis, independently powered and controlled, and usually an idle caster wheel forms a tripod-like support structure for the body of the robot. In Epi.q robots the driven wheels are substituted by driving units and the Epi.q vertical joint accomplishes the same task of the caster wheel joint, as shown in Figure 2. If both the driving units are driven in the same direction and speed, the robot goes in a straight line. If one driving unit rotates faster than the other, the robot follows a curved path, turning inward toward the slower driving unit. If one of the driving units is stopped while the other continues to turn, the robot pivots around the stopped driving unit. If the driving units turn at equal speed but in opposite directions, both driving units traverse a circular path around a point centered half way between the two driving units, therefore the forecarriage pivots around the vertical axis.
For a classic differential steering robot, shown in Figure 2 on the left, when the velocities of the two driven wheels are chosen, the position of the instantaneous center of rotation is fixed too:

$$\frac{v_{fl}}{d + i/2} = \frac{v_{fr}}{d - i/2} \tag{1}$$

Classic differential steering robot

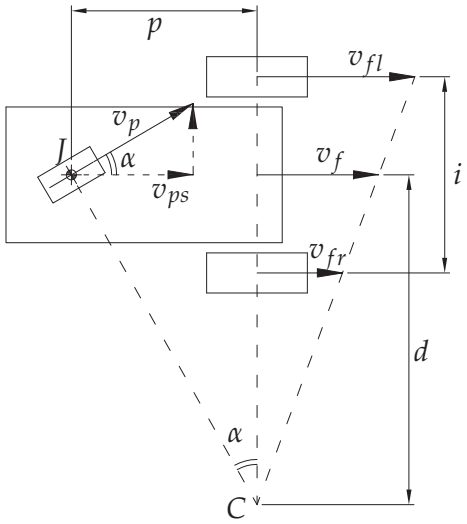

Epi.q robot

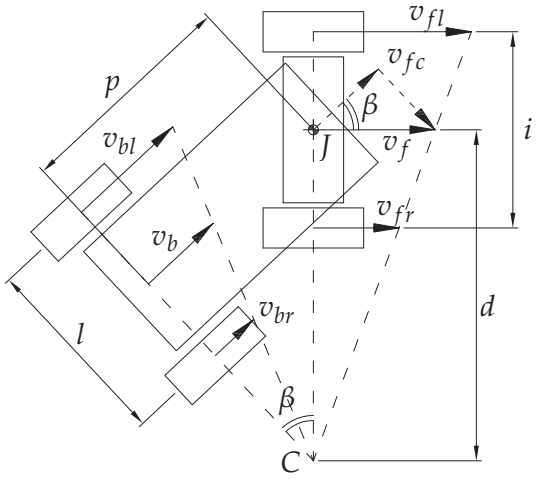

Fig. 2. Differential steering systems

$$d = \frac{v_{fl} + v_{fr}}{v_{fl} - v_{fr}} \cdot \frac{i}{2} \tag{2}$$

Consequently the velocity of a point centered half way between the two wheels is known:

$$v_f = \frac{v_{fl} + v_{fr}}{2} \tag{3}$$

and this velocity is equal to the component of the caster wheel velocity in the motion direction, otherwise there would be a deformation into robot body. During this operation the idle caster wheel is positioned by kinematic conditions and turns until it becomes orthogonal to the segment that links J and C; its velocity is a function of the driven wheel velocities:

$$v_p = \frac{v_{fl} + v_{fr}}{2\cos\alpha} \tag{4}$$

where

$$\alpha = \arctan\frac{p}{d} \tag{5}$$

For an Epi.q robot, shown in Figure 2 on the right, the mathematical treatment is quite similar. When the velocities of the two driving units are chosen, the position of the instantaneous center of rotation is fixed too:

$$\frac{v_{fl}}{d + i/2} = \frac{v_{fr}}{d - i/2} \tag{6}$$

$$d = \frac{v_{fl} + v_{fr}}{v_{fl} - v_{fr}} \cdot \frac{i}{2} \tag{7}$$

Therefore the velocity of a point centered half way between the two driving units is known:

$$v_f = \frac{v_{fl} + v_{fr}}{2} \tag{8}$$

and this point coincides with the vertical revolute joint. An angle between front and rear part of the robot is generated by kinematic conditions, that position the rear wheel unit axis in

order to pass through the instantaneous center of rotation C. The component of the vertical joint velocity in rear axle direction is equal to the rear axle velocity, otherwise there would be a deformation of the robot central body:

$$v_b = \frac{v_{fl} + v_{fr}}{2} \cos\beta \tag{9}$$

where

$$\beta = \arcsin\frac{p}{d} \tag{10}$$

and consequently the velocity of the two rear idle wheel units are:

$$v_{bl} = \frac{v_{fl} + v_{fr}}{2} \cdot \frac{d\cos\beta + l/2}{d} \tag{11}$$

$$v_{br} = \frac{v_{fl} + v_{fr}}{2} \cdot \frac{d\cos\beta - l/2}{d} \tag{12}$$

2.2 Multi-leg wheel unit

A multi-leg wheel unit consists of a plurality of radially located spokes that end with a wheel. Both the forecarriage and the rear axle employ multi-leg wheel units.

A multi-leg wheel unit has a plurality of equally spaced wheels. If the number of wheels increases, the polygon defined by the wheel centers tends to become a circle and its side length decreases; thus the step overcoming capability is reduced but, on the other hand, the rotating leg motion is improved in terms of motion smoothness. Epi.q robots employ a three-legged wheel unit because it maximizes the step overcoming capability, for a given driving unit height, and the motion smoothness is guaranteed due to the fact that these robots use wheels whenever possible and legs only when needed.

Although a multi-leg wheel unit generates more friction than a single wheel during steering operations, this solution is advantageous: when the robot is moving on uneven terrain, actually its pitching is significantly reduced; when it is facing an obstacle, actually a multi-leg wheel unit can climb over higher obstacles and generally the velocity component in motion direction of the wheel unit presents smaller discontinuities.

When Epi.q robots are moving on rough ground their body vertical displacement is significantly decreased with respect to a robot that uses single wheels. Actually, as illustrated in Figure 3, if h_o is the height of an obstacle small enough to be contained between the wheels of a three-legged wheel unit, the height of the wheel unit axis can be expressed as:

$$h_a{}' = l_l \sin 30^\circ + r_{du} \tag{13}$$

$$h_a{}'' = l_l \sin(30^\circ + \alpha) + r_{du} \tag{14}$$

The inclination α of the wheel unit can be related with the obstacle height:

$$2l_l \cos 30^\circ \sin\alpha = h_o \tag{15}$$

therefore the vertical displacement Δh_{du} of a three-legged wheel unit follows from Equations 13, 14 and 15:

$$\Delta h_{du} = h_a{}'' - h_a{}' = l_l \sin 30^\circ \cos\alpha + l_l \cos 30^\circ \sin\alpha - l_l \sin 30^\circ = \\ = \frac{h_o}{2} - \frac{l_l}{2}(1 - \cos\alpha) \tag{16}$$

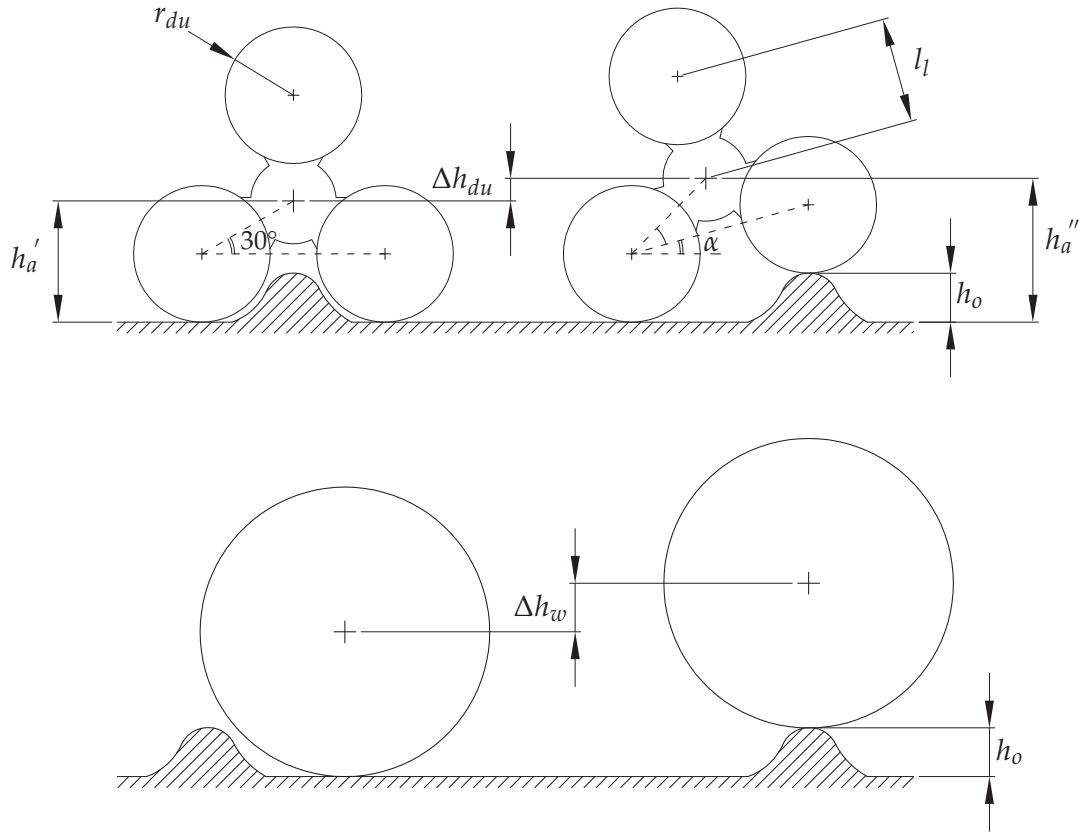

Fig. 3. Vertical displacement in presence of little unevenness, a comparative sketch between a three-legged wheel unit and a single wheel with same overall dimensions

that is always smaller or equal to half obstacle height:

$$\Delta h_{du} \leq \frac{h_o}{2} \tag{17}$$

while the vertical displacement of a single wheel, Δh_w, is always equal to obstacle height. Consequently, when the robot is moving on uneven terrain the pitching is significantly reduced with the use of a three-legged wheel unit instead of a single wheel.
As regards the ability of climbing an obstacle, a multi-leg wheel unit can climb over higher steps than a single wheel with the same overall dimensions actually, as shown in Figure 4, the maximum step that a single wheel can climb over measures a fraction of its radius while, for a multi-leg wheel unit, it is a fraction of its height: for example it was experimentally testes that the Epi.q-2 driving unit can climb over obstacles that measure till 84% of its height, see Section 4.
In case of steps that can be overcome both by a multi-leg wheel unit or by a single wheel, generally the velocity component in the motion direction presents smaller discontinuities with the multi-leg wheel unit than with a single wheel. Considering a three-legged wheel unit and a single wheel with same overall dimensions that are advancing at the same speed, shown in Figure 4, it is possible to identify a β angle:

$$\sin\beta = 1 - \frac{h_o}{r_w} \tag{18}$$

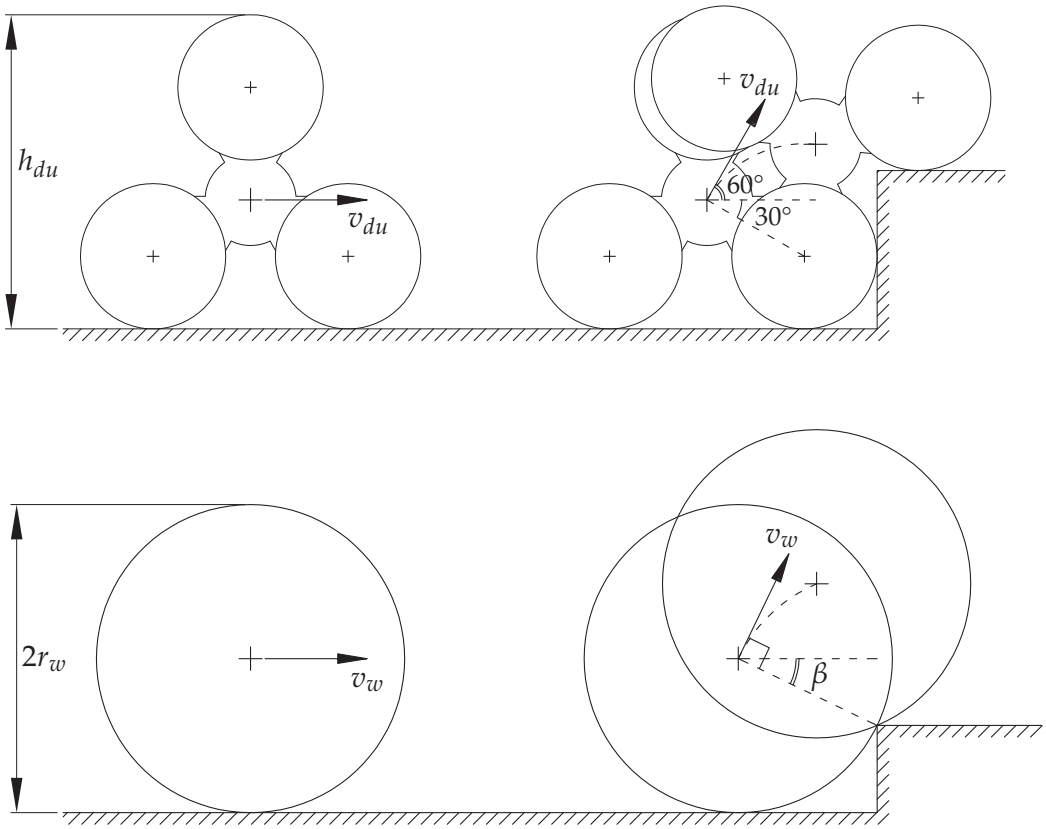

Fig. 4. Step climbing, a comparative sketch between a three-legged wheel unit and a single wheel, with same overall dimensions

The horizontal component of the wheel unit speed presents smaller discontinuities then a single wheel if the β angle is lower than 30°, that means when the obstacle is higher than a quarter of the wheel unit height or, equivalently, half wheel radius:

$$h_o > h_{du}/4 \tag{19}$$

$$h_o > r_w/2 \tag{20}$$

Moreover this discontinuity is also reduced on driving units by the fact that Epi.q robots have different velocities when they are moving on wheels or on legs, even if the gear-motors still continue to rotate at the same speed, as it will be explained in Section 3.

3. Driving unit

In this section a special focus on driving unit is discussed. The driving unit is a three-legged wheel unit having three radially located wheels, mounted at the end of each spoke. The driving units, housing the transmission system, control robot locomotion.

The driving unit concept takes place from the idea that a robot can passively modify its locomotion, from rolling on wheels to stepping on rotating legs, simply according to local friction and dynamic conditions. Actually, the driving unit is designed to have a limit torque that triggers different locomotions: if the torque required for moving on wheels exceeds the torque required for moving on legs, the robot will change its locomotion accordingly, from

rolling on wheels to stepping on legs and vice versa. Thus only one motor per driving unit is required both for wheeled and legged locomotion.

3.1 Driving unit kinematic analysis

Considering the driving unit as a planar mechanism, angularly it has two degrees of freedom: the angular position of the driving unit frame and the angular position of the wheels. Actually,

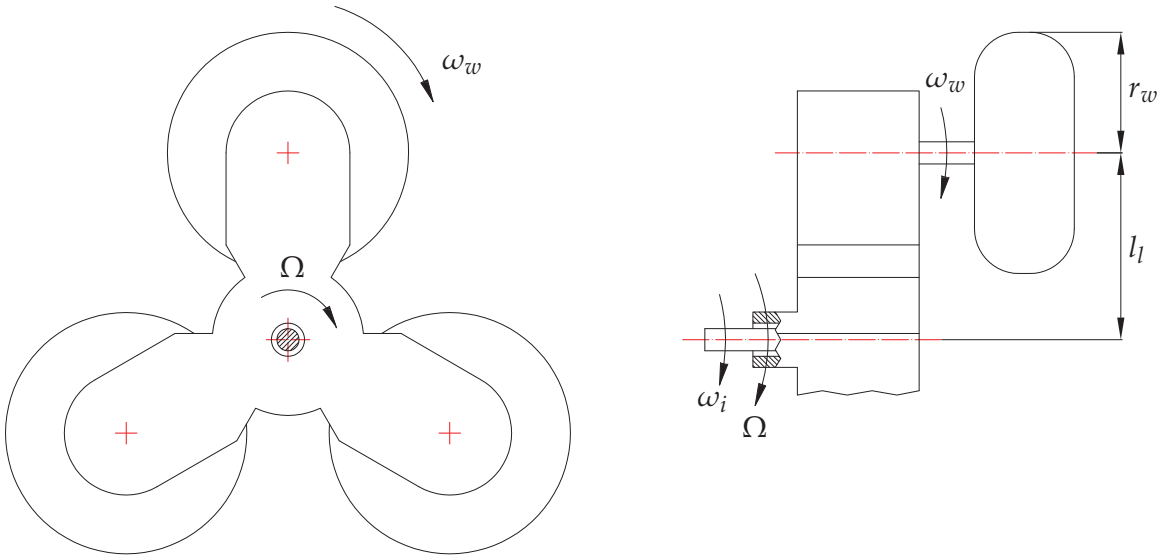

Fig. 5. Driving unit scheme

the transmission system links the input shaft angular velocity ω_i with both the angular velocity of the driving unit frame Ω, and the angular velocity of the wheels ω_w, that is the same for all the three wheels since the transmission system has the same gear ratio along each leg. Considering an observer placed on the driving unit frame, the transmission system is seen as an ordinary gearing, therefore the gear ratio (with sign) of the driving unit transmission system k_{ts} can be easily expressed as follows:

$$\frac{\omega_w - \Omega}{\omega_i - \Omega} = k_{ts} \tag{21}$$

and making ω_i explicit, it becomes:

$$\omega_i = \frac{1}{k_{ts}}\,\omega_w + \frac{k_{ts} - 1}{k_{ts}}\,\Omega \tag{22}$$

When the robot is moving on wheels, *advancing mode*, the robot weight and the contact between wheels and ground constrain driving unit angular position.
If the robot is moving on a flat ground, the driving unit angular velocity is null:

$$\Omega = 0 \tag{23}$$

therefore Equations 21 and 23 lead to identify the velocity ratio i_{ad} and the driving unit linear velocity v_a, shown in Figure 6, as follows:

$$i_{ad} = \left.\frac{\omega_w}{\omega_i}\right|_{\Omega=0} = k_{ts} \tag{24}$$

$$v_{ad} = \omega_w \cdot r_w = \omega_i \cdot i_{ad} \cdot r_w = \omega_i \cdot k_{ts} \cdot r_w \tag{25}$$

where r_w is wheel radius.
When the robot bumps against an obstacle, if the local frictions between front wheel and obstacle are sufficient to stop the wheel, the driving unit starts to rotate around the stopped wheel center, allowing the robot to climb over the obstacle, *automatic climbing mode*. In this occurrence the wheel angular velocity is null:

$$\omega_w = 0 \tag{26}$$

and consequently, from Equations 21 and 26, the velocity ratio i_{ac} and the driving unit linear velocity v_{ac}, shown in Figure 6, are respectively:

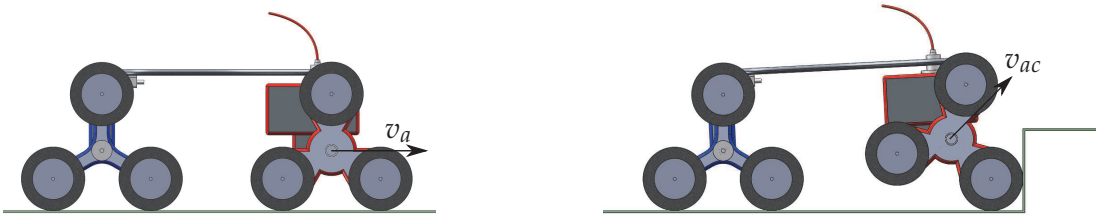

Fig. 6. Driving unit linear velocity during advancing mode, on the left, and automatic climbing mode, on the right

$$i_{ac} = \left.\frac{\Omega}{\omega_i}\right|_{\omega_w=0} = \frac{k_{ts}}{k_{ts}-1} \tag{27}$$

$$v_{ac} = \Omega \cdot l_l = \omega_i \cdot i_{ac} \cdot l_l = \omega_i \cdot \frac{k_{ts}}{k_{ts}-1} \cdot l_l \tag{28}$$

where l_l is the length of the driving unit leg.
Finally, taking into account Equations 24 and 27, it is possible to rewrite Equation 22 as follows:

$$\omega_i = \frac{\omega_w}{i_{ad}} + \frac{\Omega}{i_{ac}} \tag{29}$$

3.2 Driving unit design

During the design phase it is important to establish the correct driving unit parameters, for this reason some preliminary reflections can be helpful.
The locomotion transition between wheeled and legged motion is only triggered by driving unit torque demand therefore, since driving unit motors must rotate in the same direction both for advancing mode and for automatic climbing mode, the driving unit will work properly only if the velocity ratios i_a and i_{ac} have the same sign. Equations 24 and 27 lead to identify a low limit value for the driving unit gear ratio:

$$k_{ts} > 1 \tag{30}$$

Consequently, a suitable transmission system has a gear ratio k_{ts} bigger than one and positive: if, for example, the chosen transmission system is only made of external toothed gears, this condition will lead to choose an odd number of gears with appropriate gear radii.
A second consideration regards robot motion continuity during the locomotion transition.

The ratio between driving unit linear velocity during advancing mode and automatic climbing mode, considering only the component parallel to the ground, can be identified by a coefficient β that, from Equations 25 and 28, can be expressed as:

$$\beta = \frac{v_{ac} \cdot \cos(60^\circ)}{v_{ad}} = \frac{1}{2(k_{ts} - 1)} \cdot \frac{l_l}{r_w} \tag{31}$$

Therefore the β coefficient contains information regard motion continuity: if this value is close to the unit value, motion continuity will be preserved.
A third consideration takes into account driving unit application. Considering driving units with similar overall dimensions, different capabilities can be obtained varying the r_w/l_l parameter, as shown in Figure 7: if the r_w/l_l value decreases, the robot will be more oriented towards legged locomotion and it will be able to climb over higher obstacles, otherwise the robot will be more oriented towards wheeled locomotion, with wheels that will better protect driving unit from shocks caused by the contact with obstacles. The highest limit value for the

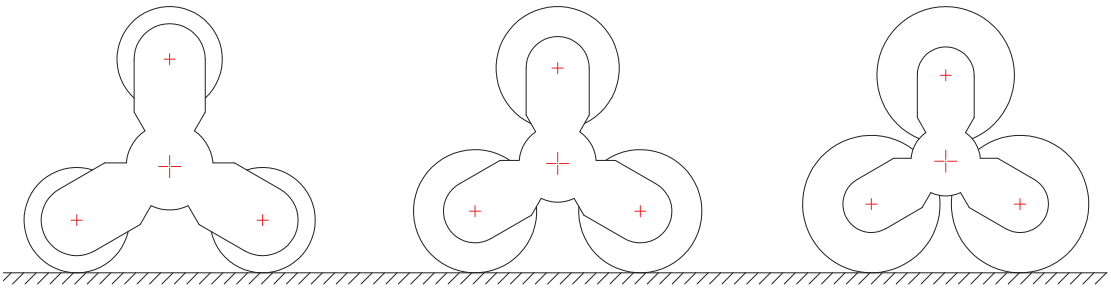

Fig. 7. Driving units with different r_w/l_l ratios, increasing value from left to right

r_w/l_l parameter corresponds to the condition in which driving unit wheels are in interference limit conditions:

$$2r_w = 2l_l \cdot \cos(30^\circ) \tag{32}$$

therefore the r_w/l_l value must be chosen accordingly to robot application and always smaller than:

$$\frac{r_w}{l_l} < \frac{\sqrt{3}}{2} \tag{33}$$

Once robot specifications are fixed and consequently the r_w/l_l and β parameters are chosen, Equation 31 identifies a first attempt value for the driving unit gear ratio:

$$k_{ts} = \frac{1}{2\beta} \cdot \frac{l_l}{r_w} + 1 \tag{34}$$

At this step it still remains to verify the predicted transition conditions between advancing mode and automatic climbing mode; if this conditions were not satisfactory, it would be necessary to relax some robot specifications.
When the gear ratio k_{ts} and the driving unit kinematic chain, as well, are chosen, lots of possible combination of mechanical components still remain to be identified: a further suggestion would be to choose the gearing that better reduce risk of interferences between driving unit frame and obstacles.
Finally, it is necessary to identify a scale factor, that will depend on the robot application field, thus the driving unit geometry is completely identified.

3.3 Epi.q-1 driving unit

The Epi.q-1 driving unit, as shown in Figures 8, is mainly composed of: an input ring gear (1) (directly linked to a gear-motor), a planet carrier (2) (rotationally free respect to robot chassis by means of bearing), three planet gears (3), a solar gear (4), a sliding solar gear (5), three leg planet gears (6), three legs (7), three planet pulleys (8), three belts (9), three wheel pulleys (10), three wheels (11), an axial device (12) linked to a mini-motor (13). The planet pulleys (8) are always rigidly connected with the planet gears (3), the wheel pulleys (10) with the wheels (11) and the leg planet gears (6) with the legs (7). An axial device controls the axial position of the

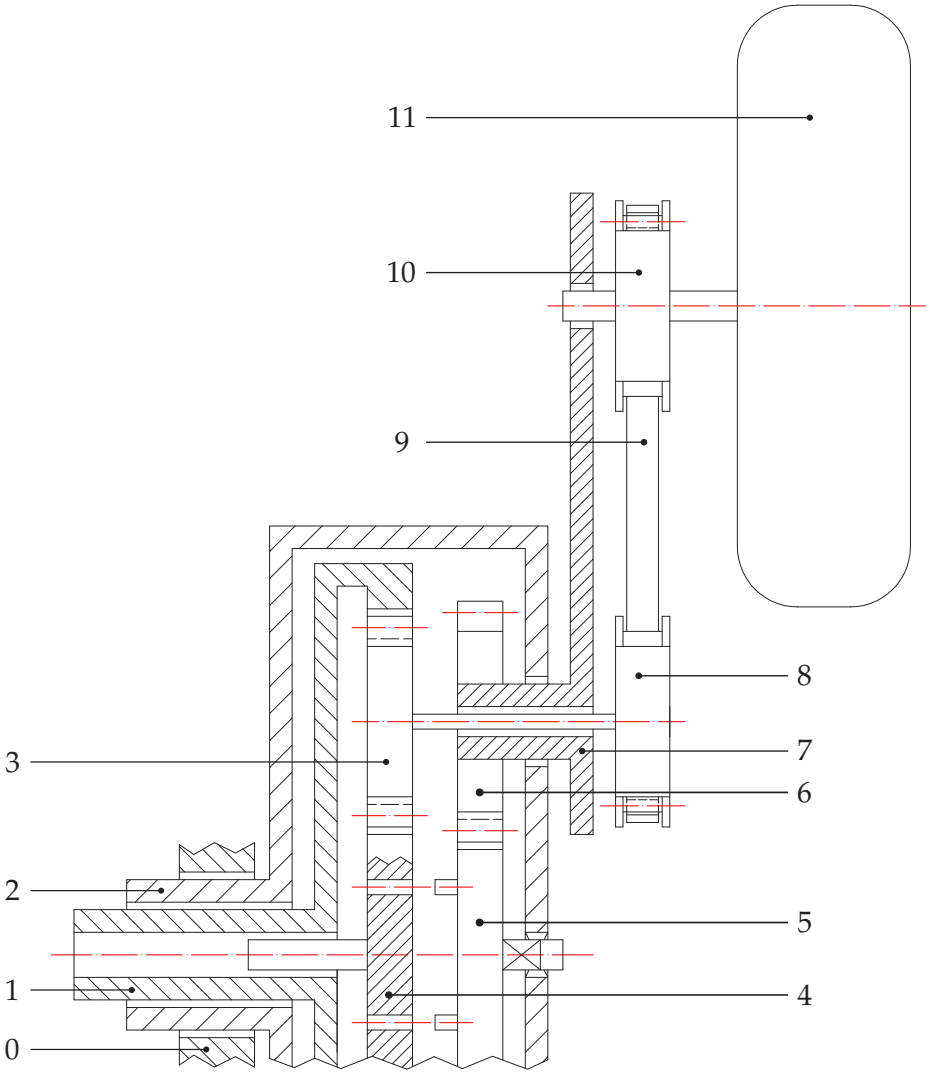

Fig. 8. Functional scheme of the Epi.q-1 driving unit, only one arm is represented

sliding solar gear (5) in order to alternatively link the leg planet gear (6) with the planet carrier (2) or with the solar gear (4), as shown in Figure 9

The operative conditions of the transmission system can be described using some kinematic equations: some of them are always valid for every operative conditions, three represent the

Nomenclature	Radius	Rot. speed	Label
Chassis			0
Input ring gear	r_r	ω_r	1
Planet carrier		Ω	2
Planet gears	r_p	ω_p	3
Solar gear	r_s	ω_s	4
Sliding solar gear	r_{ss}	ω_{ss}	5
Leg planet gears	r_{lp}	ω_l	6
Legs		ω_l	7
Planet pulleys	r_{pp}	ω_p	8
Toothed belts			9
Wheel pulleys	r_{wp}	ω_w	10
Wheels	r_w	ω_w	11

Table 1. Nomenclature of Epi.q-1 driving unit

meshing conditions in the epicyclic gearing:

$$\frac{\omega_p - \Omega}{\omega_r - \Omega} = +\frac{r_r}{r_p} = k_{e1} \tag{35}$$

$$\frac{\omega_s - \Omega}{\omega_p - \Omega} = -\frac{r_p}{r_s} = k_{e2} \tag{36}$$

$$\frac{\omega_l - \Omega}{\omega_{ss} - \Omega} = -\frac{r_{ss}}{r_{lp}} = k_{el} \tag{37}$$

while a fourth one describes the belt transmission system:

$$\frac{\omega_w - \omega_l}{\omega_p - \omega_l} = +\frac{r_{pp}}{r_{wp}} = k_b \tag{38}$$

Moreover the gear ratii k_{e1} and k_{e2} are linked by geometrical constraints:

$$r_r = r_s + 2r_p$$

$$\frac{r_r}{r_p} = \frac{r_s}{r_p} + 2$$

therefore:

$$k_{e2} = \frac{1}{2 - k_{e1}} \tag{39}$$

Other equations, describing physical constraints introduced by the sliding solar gear meshing conditions and by robot-terrain contact, are univocally determined by robot operative conditions; these equations will be introduced in the following.

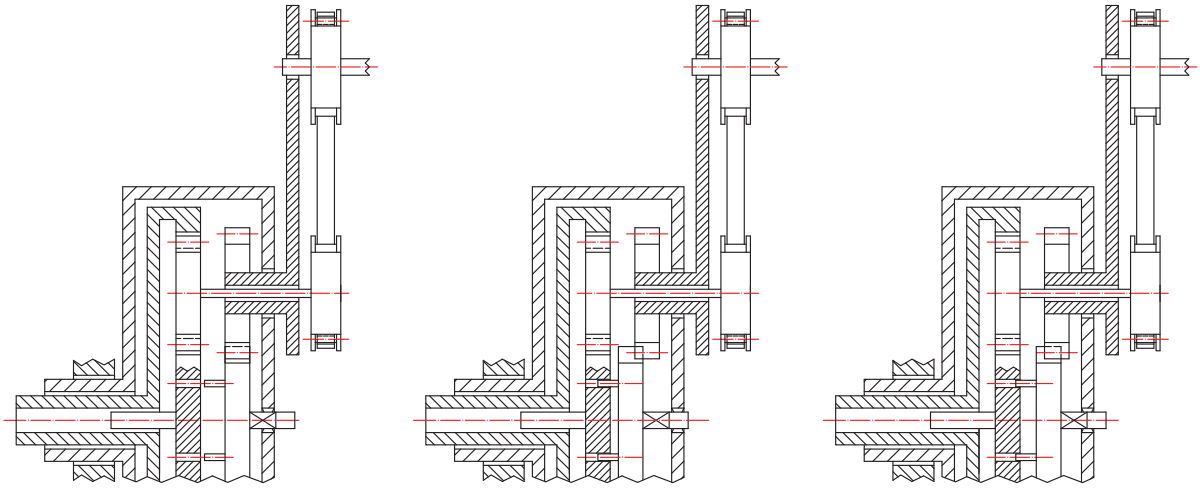

Fig. 9. Driving unit configurations for different operative modes: advancing and automatic climbing modes (on the left); changing configuration mode (in the middle); rotating leg mode (on the right)

3.3.1 Advancing & automatic climbing modes

During advancing mode the robot weight and the contact between bottom wheels and ground constrain driving unit angular position. When the robot bumps against an obstacle, if the local frictions between front wheel and obstacle are sufficient to stop the wheel, the driving unit starts to rotate around that wheel, automatic climbing mode, allowing the robot to climb over the obstacle. The robot passively changes its locomotion simply according to the torque required.

In both advancing mode and automatic climbing mode, the sliding solar gear (5) is prismatically coupled with the planet carrier (2), so that a relative rotation between them is hindered, as shown in Figure 9 on the left. The sliding solar gear (5) is always meshed with the leg planet gears (6), in order to prevent a relative rotation between legs (7) and planet carrier (2), this way legs (7) are locked to the planet carrier (2) in a prefixed position.

Advancing mode

In advancing mode the robot is moving with its legs rigidly connected to the planet carrier, actually the sliding solar gear is coupled with the planet carrier:

$$\omega_{ss} = \Omega \tag{40}$$

and it meshes with the leg planet gears, therefore:

$$\omega_l = \Omega \tag{41}$$

The planet carrier is free to rotate around its axis, but the driving unit balance and the contact between wheels and ground constrain its angular position. In the hypothesis of locomotion on flat ground, the contact between wheels and ground hinders planet carrier rotation:

$$\Omega = 0 \tag{42}$$

Equations from 35 to 42 lead to identify the advancing velocity ratio i_a and the robot speed in advancing mode v_a as a function of the gear-motor rotation speed:

$$i_{ad} = \left.\frac{\omega_w}{\omega_m}\right|_{\Omega=0} = k_{e1} \cdot k_b \tag{43}$$

$$v_a = \omega_w \cdot r_w = \omega_r \cdot i_{ad} \cdot r_w = \omega_m \cdot k_{e1} \cdot k_b \cdot r_w \tag{44}$$

where ω_m is the angular velocity of the gear-motor output shaft, directly linked to the input ring gear.
Comparing Equations 43 and 44 with the generic Equations 24 and 25, a relationship between gear ratios can be established:

$$k_{ts} = k_{e1} \cdot k_b \tag{45}$$

Summary: during the advancing mode the sliding solar gear is coupled with the planet carrier; the motion is transferred from the gear-motor to the wheels; the planet carrier is free to swing, reducing this way robot pitching.

Automatic climbing mode
In automatic climbing mode, since the sliding solar gear is still rigidly connected with the planet carrier, the robot is still moving with its legs rigidly connected to the planet carrier, as previously described for the advancing mode, therefore Equations 40 and 41 are still available:

$$\omega_{ss} = \Omega$$
$$\omega_l = \Omega$$

Certainly, also the planet carrier is still free to rotate around its axis but, in automatic climbing mode, the local friction between front wheel and obstacle is sufficient to block the wheel in contact with the obstacle, therefore:

$$\omega_w = 0 \tag{46}$$

Equations from 35 to 41, together with 46 allow to evaluate the planet carrier angular speed:

$$\Omega = \frac{k_{e1} \cdot k_b}{k_{e1} \cdot k_b - 1} \cdot \omega_m \tag{47}$$

thus the automatic climbing velocity ratio i_{ac} and the driving unit velocity in automatic climbing mode v_{ac} can be expressed as follows:

$$i_{ac} = \left. \frac{\Omega}{\omega_m} \right|_{\omega_w = 0} = \frac{k_{e1} \cdot k_b}{k_{e1} \cdot k_b - 1} \tag{48}$$

$$v_{ac} = \Omega \cdot l_l = \omega_m \cdot \frac{k_{e1} \cdot k_b}{k_{e1} \cdot k_b - 1} \cdot l_l \tag{49}$$

that compared with Equations 27 and 28 lead to:

$$k_{ts} = k_{e1} \cdot k_b \tag{50}$$

as it was expected, confirming Equation 45.

Summary: during the automatic climbing mode the sliding solar gear is coupled with the planet carrier; the front wheel in contact with the obstacle is stopped by the friction forces due to the contact between wheel and obstacle themselves; the whole driving unit rotates around the stopped wheel, traversing the step.

3.3.2 Changing configuration mode

Driving unit can also modify its geometry from a closed configuration to an open one, as shown in Figure 10. The closed configuration is suitable to reach restricted spaces while the open one to get over obstacles.
In *changing configuration mode* the sliding solar gear (5) is no longer engaged in the planet carrier (2) whereas it is shifted towards the solar gear (4) and coupled with it, as shown Figure 9 in the middle, therefore:

$$\omega_{ss} = \omega_s \tag{51}$$

In order to avoid gearing lability this operation is split into two steps: first the sliding solar gear (5) couples with the solar gear (4), then the sliding solar gear (5) is rotationally disconnected from the planet carrier (2). A slow solar gear rotation and some elastic elements allow a correct axial engagement between the sliding solar gear (5) and solar gear (4) fittings. During the changing configuration mode the planet carrier angular speed is null:

$$\Omega = 0 \tag{52}$$

Therefore Equations from 35 to 38, together with 51 and 52, bring to evaluate the changing configuration velocity ratio as:

$$i_{cc} = \frac{\omega_l}{\omega_m} = k_{e1} \cdot k_{e2} \cdot k_{el} = \frac{k_{e1}\, k_b}{2 - k_{e1}} \tag{53}$$

Legs angular excursion is limited by suitable mechanical stops, placed on the planet carrier.
A relative slippage between wheels and ground can happen during the changing configuration operations.

Summary: during the changing configuration mode the sliding solar gear is shifted and coupled with the solar gear; the planet carrier is blocked; the motion is transferred from the gear-motor to the legs, that rotate.

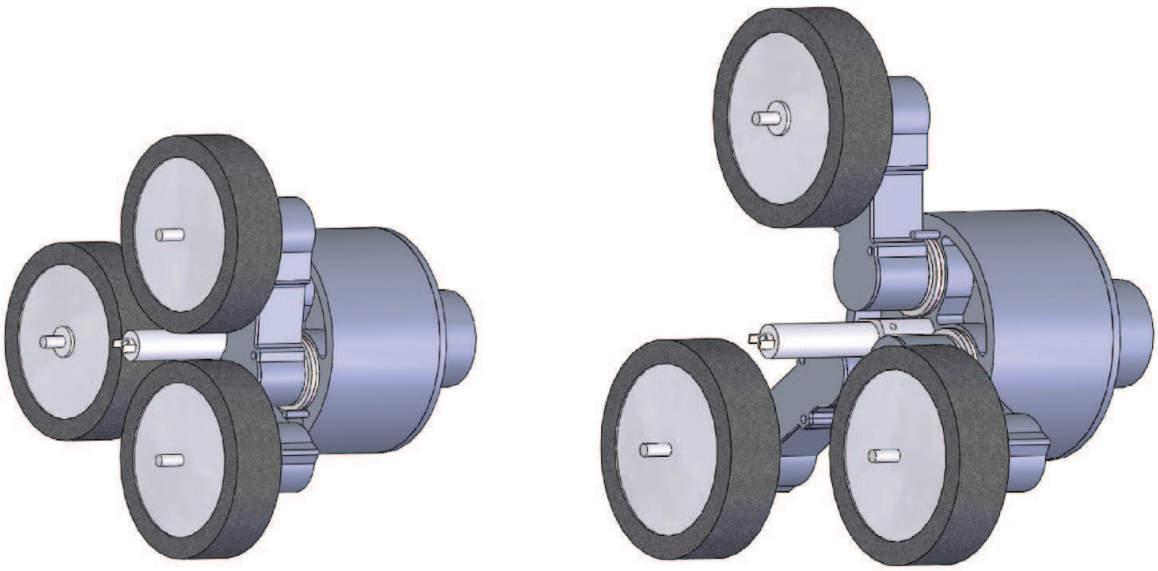

Fig. 10. Driving unit in closed and in open configuration

3.3.3 Rotating leg mode

When the robot cannot climb an obstacle in automatic climbing mode, due for example to a low friction coefficient between wheel and obstacle, it is possible to transform the driving unit into a whole rigid body which rotates around its axis, *rotating leg mode*.
Figure 9 on the right shows gearing configuration for this operative mode: the sliding solar gear (5) is shifted into an intermediate position in order to be simultaneously engaged with both the solar gear (4) and the planet carrier (2):

$$\omega_{ss} = \omega_s = \omega_l = \Omega \tag{54}$$

Equations from 35 to 38 together with 54 allow to evaluate the driving unit angular speed as follows:

$$\Omega = \omega_m \tag{55}$$

Actually, the driving unit acts as a rigid body and the motor rotation provides the rotation of the whole driving unit, as it was a single rotating body.
Wheels wear is a possible drawback of this locomotion when slipping conditions between wheel and obstacle occur.

Summary: during the rotating leg mode the sliding solar gear (5) is shifted into an intermediate position; the whole driving unit rotates as a rigid body around its central axis.

3.4 Epi.q-2 driving unit

The driving unit implemented in Epi.q-2 prototype is shown in Figure 11. With respect to Epi.q-1 version, the changing configuration ability has been removed in order to simplify the structure, to increase gearing robustness and efficiency, and to reduce overall weight.
The driving unit, as shown in Figure 11, consists of: an input solar gear (1), a planet carrier (2)

Nomenclature	**Radius**	**Rot. speed**	**Label**
Frame			0
Input Solar gear	r_s	ω_s	1
Planet carrier	l_l	Ω	2
First planet gear	r_{fp}	ω_{fp}	3
Second planet gear	r_{sp}	ω_w	4
Wheel	r_w	ω_w	5

Table 2. Nomenclature of Epi.q-2 driving unit

(rotational free respect to robot frame by means of bearings), three first planet gears (3), three second planet gears (4) and three wheels (5).
The transmission system can be described using some kinematic equations; the meshing conditions in the epicyclic gearing can be represented as follows:

$$\frac{\omega_{fp} - \Omega}{\omega_s - \Omega} = -\frac{r_s}{r_{fp}} = k_{e1} \tag{56}$$

$$\frac{\omega_w - \Omega}{\omega_{fp} - \Omega} = -\frac{r_{fp}}{r_{sp}} = k_{e2} \tag{57}$$

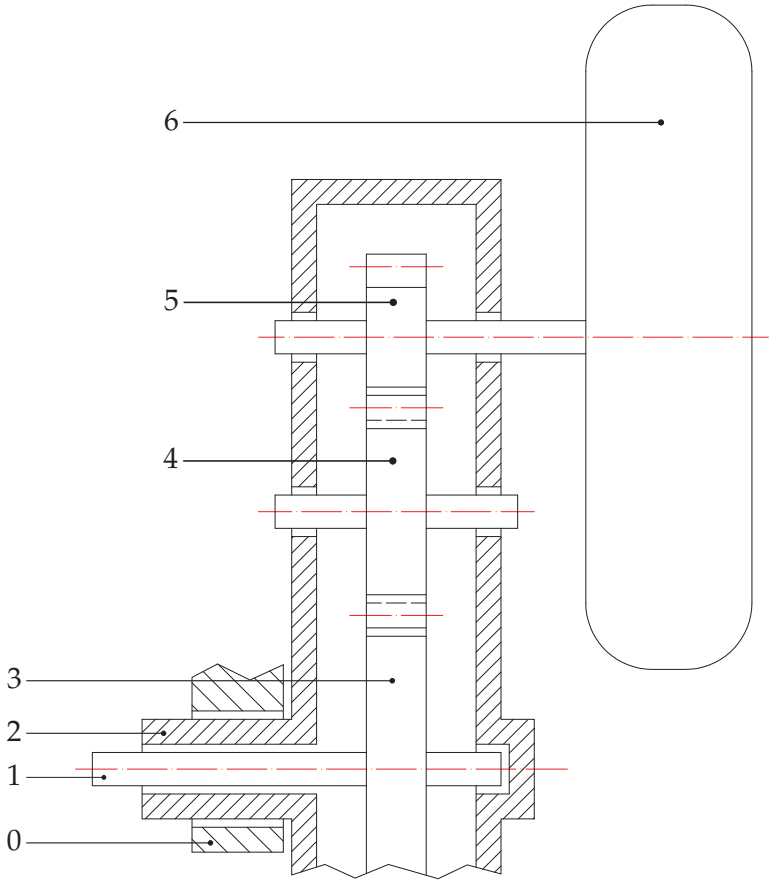

Fig. 11. Epi.q-2 driving unit

During advancing mode the robot weight and the contact between bottom wheels and ground constrain driving unit angular position.

$$\Omega = 0 \tag{58}$$

In this occurrence the velocity ratio i_a and the robot linear velocity v_a, from Equations 56, 57 and 58, are respectively:

$$i_{ad} = \left. \frac{\omega_w}{\omega_s} \right| \Omega = 0 = k_{e1} \cdot k_{e2} \tag{59}$$

$$v_{ad} = \omega_w \cdot r_w = \omega_s \cdot i_{ad} \cdot r_w = \omega_m \cdot k_r \cdot k_{ts} \cdot r_w \tag{60}$$

where k_r is the reducer gearing ratio, located between driving unit input shaft and motor, and ω_m is the angular velocity of the motor output shaft.
Comparing the Equations 59 and 60 with the generic Equations 24 and 25, it is possible to establish a relationship between gear ratii:

$$k_{ts} = k_{e1} \cdot k_{e2} \tag{61}$$

When the robot bumps against an obstacle, if the local frictions between front wheel and obstacle are sufficient to stop that wheel:

$$\omega_w = 0 \tag{62}$$

then the second planet gear rotation is hindered and consequently the driving unit rotation starts around the stopped wheel, allowing the robot to climb over the obstacle.
In this occurrence the gear ratio i_{ac} and the robot linear velocity v_{ac} are respectively:

$$i_{ac} = \frac{\Omega}{\omega_s}\bigg|\, \omega_w = 0 = \frac{k_{e1} \cdot k_{e2}}{k_{e1} \cdot k_{e2} - 1} \tag{63}$$

$$v_{ac} = \Omega \cdot l_l = \omega_s \cdot i_{ac} \cdot l_l = \omega_s \cdot \frac{k_{e1} \cdot k_{e2}}{k_{e1} \cdot k_{e2} - 1} \cdot l_l \tag{64}$$

that compared with Equations 27 and 28 lead to:

$$k_{ts} = k_{e1} \cdot k_{e2} \tag{65}$$

as it was expected, confirming Equation 61.

4. Tests

Epi.q robots move well on different terrains: from a structured environment, with flat surface and steps, to an unstructured one, with uneven ground and obstacles different in dimension and shape.
When the robot is moving on wheels in advancing mode, the robot weight and the contact between the bottom wheels and the ground constrains driving unit angular position, as shown in Figure 12; actually the driving units are axially joined to the forecarriage frame but

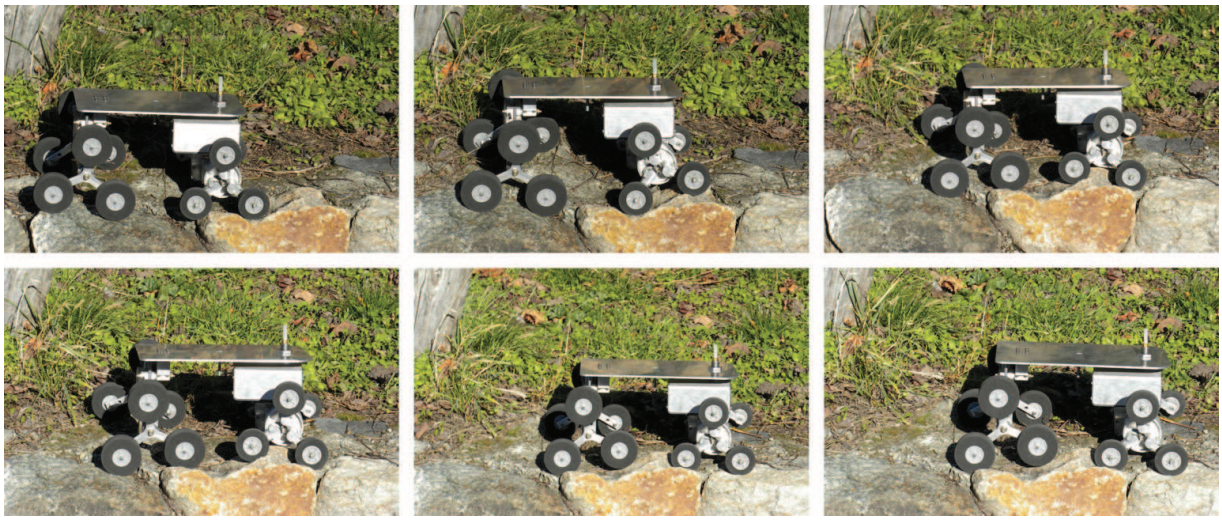

Fig. 12. Epi.q-1 in advancing mode, on uneven ground

rotationally free by means of bearings. When the robot bumps against an obstacle, if the local frictions between front wheel and obstacle are sufficient to stop that wheel, the driving unit starts to rotate around the stopped wheel center, allowing the robot to climb over the obstacle in automatic climbing mode, shown in Figure 13. The transition between wheeled and legged locomotion is passively triggered: if the torque required for moving on wheels is higher than

the torque required for moving on legs, the robot would change its locomotion from rolling on wheels to stepping on legs, and vice versa.
Experimental tests on Epi.q prototypes were conducted in order to assess their performance; tests and results are reported in the following sections.

Fig. 13. Epi.q-2 negotiating an obstacle

4.1 Step negotiating aptitude

The purpose of the test is to assess the ability of Epi.q robots to negotiate obstacles which are different in height. The robots were driven close to a step, on a flat surface. Analyzing the experimental tests, it was noticed that three different cases can occur when the rotation of the driving unit starts, as shown in Figure 14: the top wheel leans against the upper surface of the step; the top wheel leans against the front surface of the step; or an intermediate case between the two. In the first case it is always possible to overcome the step, even without

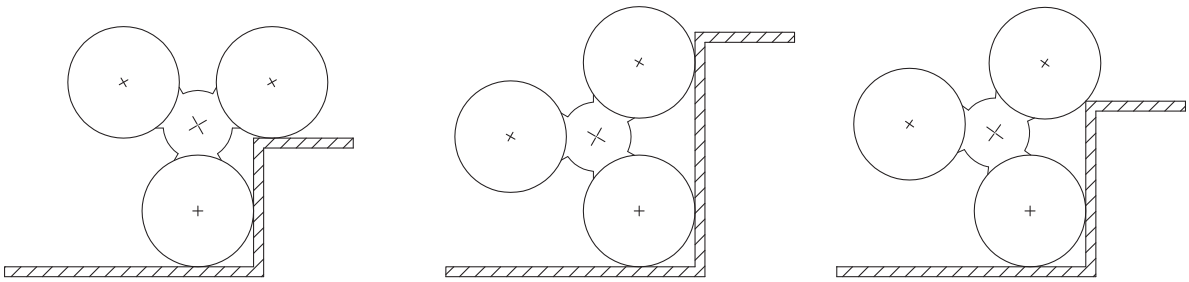

Fig. 14. Driving unit approaches three steps, different in height

initial velocity. Actually, when the rotation of the driving unit starts, the top wheel is above the step and the upper leg can lift up the robot, obviously only if the top wheel does not skid. In the second case it is never possible to overcome the step, because the rear wheel units are idle. In an intermediate case between the previous ones the possibility of overcoming a step depends on the static friction coefficient between wheels and step, on the tread pattern of the tire and on the approach speed.

4.1.1 Epi.q-1 test results

The experimental tests conducted on Epi.q-1 prototype have shown that the maximum step it can negotiate, in favourable friction conditions, is 90 mm height, equivalent to 72% of the

driving unit height.
When the driving unit was in closed configuration, Epi.q-1 crossed almost all obstacles without interference between driving unit and obstacles; actually, the driving unit was protected by the wheels.When the driving unit was in open configuration, sometimes a collision between driving unit and obstacles occurred. In this case the robot overcame the obstacles with a slightly irregular motion, combining the advancing mode and the automatic climbing mode. A step negotiating sequence is represented in Figure 15.

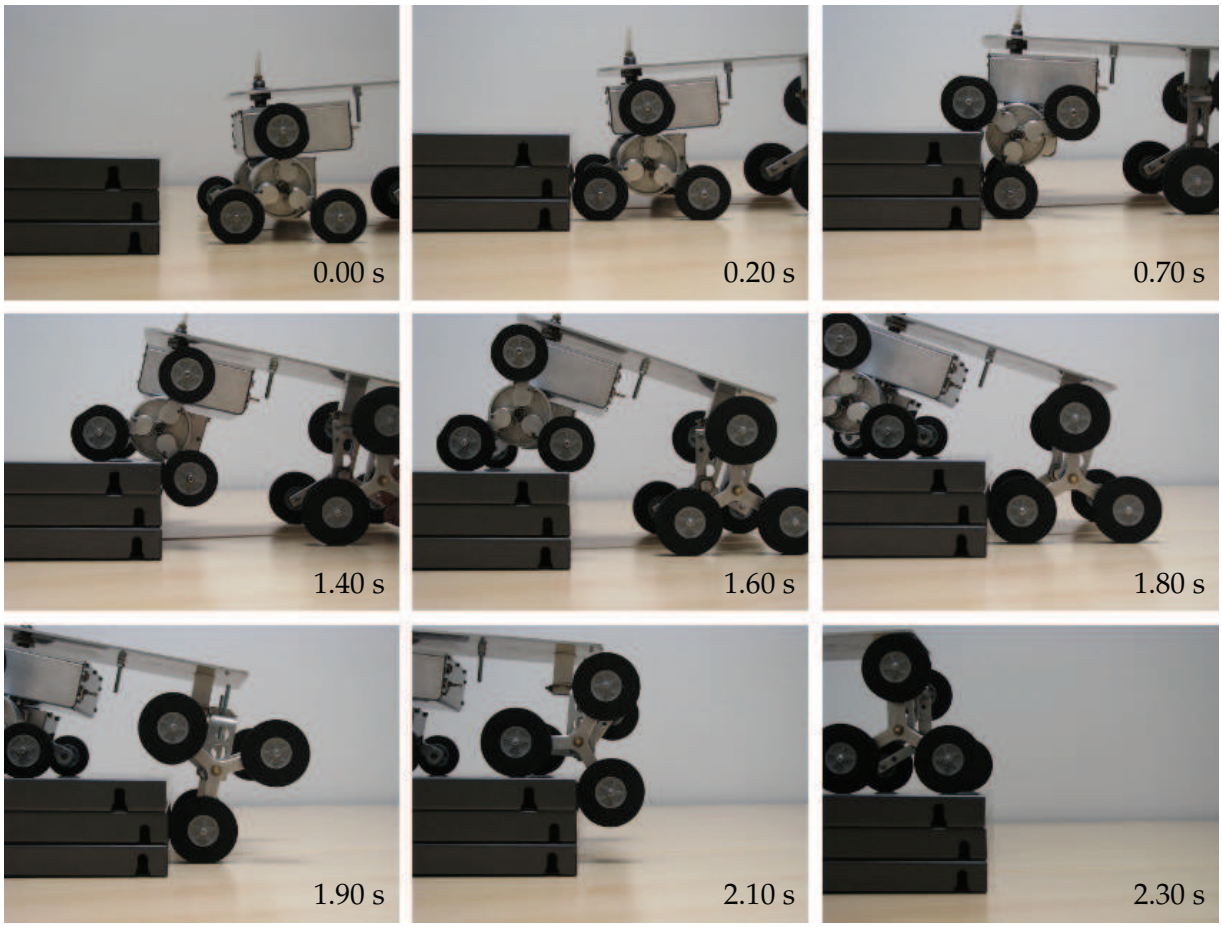

Fig. 15. Epi.q-1 negotiating a step (time stamps have been roughly estimated from a video)

4.1.2 Epi.q-2 test results

The experimental tests conducted on Epi.q-2 prototype have shown that the maximum step Epi.q-2 can climb over, in favourable friction conditions, is 110 mm height, equal to 84% of the driving unit height.
Epi.q-2 was also designed with the aim to reduce the risk of interference with obstacles; even if sometimes this condition can occur. The tests demonstrated that the robot overcomes the obstacle with a slightly irregular motion which combines the advancing mode and the automatic climbing mode.

4.2 Motion on inclined surface

The aim of the test is to assess Epi.q robot ability of moving on inclined surfaces. The robots were driven up a ramp and their behavior was observed.
The robots can drive on a slope either in advancing or in automatic climbing modes, actually there is a limit slope value that triggers the transition between wheeled and legged locomotion. Moreover there is a maximum slope value, that the robot can not overcome. This slope value is limited by motor power, by the disposition of the center of mass of the robot and by the friction coefficient between wheels and ground.
The tests highlighted a great influence of the center of mass disposition. Actually Epi.q robots does not have an active stability system and the traction is provided only by the front wheel units, which are also less loaded going uphill. Therefore, the driving units can loose traction on a slope and the wheels can start skidding.

4.2.1 Epi.q-1 test results

The experimental tests have shown that when Epi.q-1 is moving on an inclined surface the transition between advancing mode and automatic climbing mode is triggered by a 13% slope, if the the driving unit is in open configuration, and by a 9.5% slope, in case of closed configuration. The robot was tested on different surfaces with increasing friction coefficient: plexiglas, paper and plywood. When the robot is moving on plexiglas surface it can reach a slope of 29% in automatic climbing mode, if the slope is steeper the robot starts skidding while it continues to advance up to a maximum slope of 32%. When the robot moves on paper surface, the maximum slope it can reach without skidding is 40% in automatic climbing mode, but it can advance up to 43% slope. Moving on plywood the wheels never skid and the maximum slope it can reach is 45%, dur to motor torque limitations.

4.2.2 Epi.q-2 test results

The experimental tests have shown that the Epi.q-2 locomotion transition is triggered by a 31% slope. In the experimental campaign Epi.q-2 prototypes has been tested on slopes up to 33%, with friction coefficient $\mu_s = 0.83$. Obviously, when the maximum slope is limited by the friction coefficient, the traction wheels can start skidding without reaching the transition condition.

4.3 Motion on uneven and soft terrains

The purpose of the test is to assess the Epi.q robot ability of moving on different terrains.
The experimental tests have shown that, when the rotation of the wheels is hindered by the high rolling friction due to the grass or to the ground unevenness, the transition between advancing mode and automatic climbing mode occurs and the robot starts the legged locomotion, as expected.
The Epi.q robots were tested on different scenarios: on uneven terrains with grass, stones, pebbles, earth and irregular trails. In all cases they were able to advance with a motion that changed between advancing mode and automatic climbing mode: the percentage of automatic climbing mode became higher accordingly to the terrain unevenness.

4.4 Energy demand

The purpose of the test is to evaluate the energy demand of Epi.q robots. Actually, using wheels whenever possible and legs only when needed, They should require a small amount of energy.

The Epi.q-2 prototype was tested on a smooth terrain, the current demand and the speed were evaluated; the results are collected in Table 3.

Current	Speed
0.4 A	0.2 m s^{-1}
0.5 A	0.5 m s^{-1}
0.6 A	0.75 m s^{-1}

Table 3. Epi.q-2 current demand, moving on smooth terrain at different speeds

The Epi.q-2 power source, both for motor and electronics, was a removable 11 V/2200 mA h lithium-ion battery, providing more than 4 hours continuous runtime on one charge, up to 6 km of travel.

5. Technical specifications

5.1 Epi.q-1 technical specifications

Epi.q-1 weighs almost 2.6 kg and measures 160 mm × 360 mm × 280 mm (height × length × width), with a driving unit that measures 125 mm in height in open configuration and 98 mm in closed configuration.
Epi.q-1 can go up and down stairs and climb over obstacles with a maximum height of 90 mm, that is 72% of the driving unit height, as shown in Figure 16.

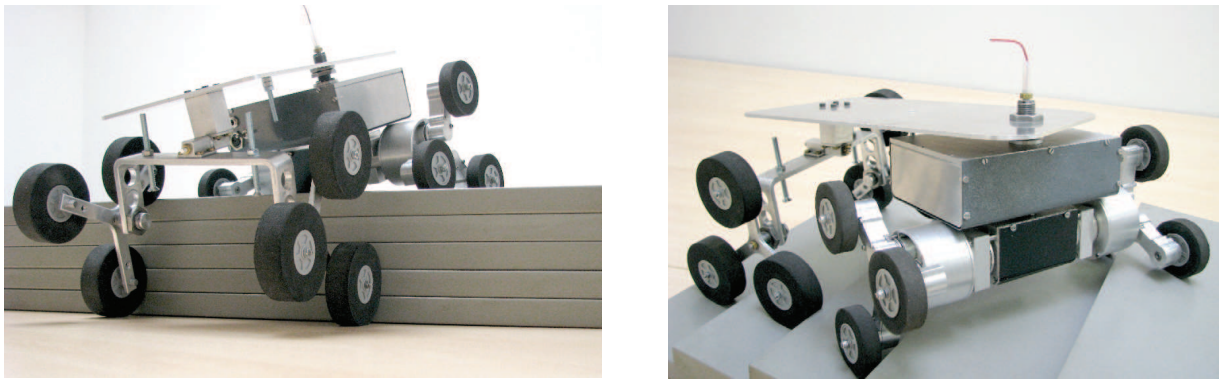

Fig. 16. Epi.q-1 traversing obstacle and stairs

On flat ground the maximum speed it can reach is approximately 0.5 m s^{-1}. On a slope, the theoretical maximum value it can drive (maximum gravitational stability margins) is limited to 62° when the robot is moving uphill frontwards (or downhill backwards), to 32° when it is moving downhill frontwards (or uphill backwards), and to 59° when it is driving along a cross-hill (or normal to a downhill). When the robot is driving uphill, the maximum slope value is limited to 20°, due to motor torque limitation.
Each driving unit is powered by a *Solarbotics GM17* gear-motor, declared specifications are a no load angular speed of 60 rpm and a maximum torque of almost 1 N m, when it is powered at 12 V. The axial device is powered by a *Faulhaber DC-micromotor* (series 0816) combined with a compatible planetary gearhead (series 08/01). The human operator controls the robot by means of an *Hitec - Laser 4* transmitter, and the radio signal is processed by a *Sabertooth 2X5* driver that provides the motors with the proper voltage.The power source both for motor and electronics is a removable 11 V/2200 mA h.

5.2 Epi.q-2 technical specifications

Epi.q-2 weighs almost 4 kg and measures 200 mm × 450 mm × 280 mm (height × length × width), with a driving unit that measures 130 mm in height.
Epi.q-2 can go up and down stairs and climb over obstacles with a maximum height of 110 mm, that is 84% of the driving unit height.
On flat ground the maximum speed it can reach is almost 1 m s^{-1}. On a slope, the theoretical maximum value it can drive (maximum gravitational stability margins) is limited to 70° when the robot is moving uphill frontwards (or downhill backwards), to 51° when it is moving downhill frontwards (or uphill backwards), and to 60° when it is driving along a cross-hill (or normal to a downhill). When the robot is driving uphill, the maximum slope value is limited to 15°, due to motor torque limitation.

Fig. 17. Epi.q-2 traversing an obstacle, on uneven ground

Each driving unit is powered by a gear-motor, declared specifications are a no load angular speed of about 81 rpm and a maximum torque of almost 0.5 N m, when it is powered at 12 V. The human operator controls the robot by means of a *Zebra 4* transmitter, and the radio signal is processed by a *Sabertooth 2X5* driver that provides the motors with the proper voltage. The power source both for motor and electronics is a removable 11 V/2200 mA h lithium-ion battery, providing more than 4 hours continuous runtime on one charge, up to 6 km of travel.

6. Conclusions

The paper has dealt with Epi.q robots, smart mini devices able to move in structured and unstructured environments, to climb over obstacles and to go up and down stairs. These robots do not need to actively sense obstacles for climbing them, they simply move forward and let their locomotion passively adapt to ground conditions and change accordingly: from rolling on wheels to stepping on legs and vice-versa.
Epi.q robots are mainly composed of three parts: a forecarriage, a central body and a rear axle. The forecarriage consists of a box linked to two driving units that, housing the transmission system, control robot locomotion. The rear axle comprises two idle three-legged wheel units with three idle wheels mounted at the end of each spoke. The central body is a metal platform connecting forecarriage and rear axle, where a payload can be placed. Two passive revolute joints, mutually perpendicular, link front and rear part of the robot: the vertical joint allows robot steering, while the horizontal joint guarantees a correct contact between wheels and ground, also in presence of uneven terrain. A differential steering is implemented on Epi.q robots, that provides both driving and steering functions.

Driving unit is the core of these devices. Epi.q driving unit concept takes place from the idea that a robot can passively modify its locomotion, from rolling on wheels to stepping on legs, simply according to local friction and dynamic condition. Actually, the driving unit is designed to have a limit torque that triggers different locomotion: if the torque required for moving on wheels exceeds the torque required for moving on legs, the robot changes its locomotion accordingly, from rolling on wheels to stepping on legs and vice versa. Thus only one motor per driving unit is required both for wheeled and legged locomotion. When the robot is moving on wheels, the robot weight and the contact between wheels and ground constrain driving unit angular position but, when the robot bumps against an obstacle, if the local frictions between front wheel and obstacle are sufficient to stop that wheel, the driving unit starts to rotate around the stopped wheel center, allowing the robot to climb over the obstacle.Therefore, wheels are used whenever possible and legs only when needed, consequently these robots require a small amount of energy if compared to tracked or legged robots.
Epi.q robots can be successfully employed in many fields: from monitoring and surveillance tasks to intervention in potentially dangerous environments like in presence of radiation, gas or explosive, from rescue operations after catastrophic events to exploration of unknown environments, and in many other fields as well.

7. References

Allen, T. J., Quinn, R. D., Bachmann, R. J. & Ritzman, R. E. (2003). Abstracted biological principles applied with reduced actuation improve mobility of legged vehicles, *Proceedings of the 2003 IEEE/RSJ - Int. Conference on Intelligent Robots and Systems*, Las Vegas, Nevada.

Dalvand, M. & Moghadam, M. (2006). Stair climber smart mobile robot (MSRox), *Autonomous Robots* 20(1): 3–14.

Galileo Mobility Instruments & Elbit Systems Ltd (2009). Elbit viper, Robot Magazine. `http://www.galileomobility.com/?page_id=12`.

Grand, C., Benamar, F., Plumet, F. & Bidaud, P. (2004). Stability and traction optimization of a reconfigurable wheel-legged robot, *The International Journal of Robotics Research* 23(10–11): 1041–1058.

iRobot (2010). Ground robots - 510 packbot. `http://www.irobot.com/gi/ground/510_PackBot`.

Lego Mindstorm (2007). Artic snow cat. `http://us.mindstorms.lego.com/en-us/Community/NXTLog/DisplayProject.aspx?id=c7d16dfe-780b-4b19-9aa3-3c0b22065dd5`.

Mourikis, A., Trawny, N., Roumeliotis, S., Helmick, D. & Matthies, L. (2007). Autonomous stair climbing for tracked vehicles, *The International Journal of Robotics Research* 26(7): 737–758.

Oderio, R. (2011). *Innovative concepts for stair climbing devices*, PhD thesis, Politecnico di Torino.

Poulakakis, I., Papadopoulos, E. & Buehler, M. (2006). On the stability of the passive dynamics of quadrupedal running with a bounding gait, *The International Journal of Robotics Research* 25(7): 669–687.

Poulakakis, I., Smith, J. & Buehler, M. (2005). Modeling and experiments of untethered quadrupedal running with a bound gait: the scout ii robot, *The International Journal of Robotics Research* 24(4): 239–256.

Quaglia, G., Bruzzone, L., Bozzini, G., Oderio, R. & Razzoli, R. (2011). Epi. q-tg: mobile robot for surveillance, *Industrial Robot: An International Journal* 38(3): 282–291.

Quaglia, G., Maffiodo, D., Franco, W., Appendino, S. & Oderio, R. (2010). The epi.q-1 hybrid mobile robot, *The International Journal of Robotics Research* 29(1).

Quinn, R. D., Nelson, G. M., Bachmann, R. J., Kingsley, D. A., Offi, J. T., Allen, T. J. & Ritzmann, R. E. (2003). Parallel complementary strategies for implementing biological principles into mobile robots, *The International Journal of Robotics Research* 22(3-4): 169–186.

Saranli, U., Buehler, M. & Koditschek, D. (2001). Rhex: A simple and highly mobile hexapod robot, *The International Journal of Robotics Research* 20(7): 616–631.

Saranli, U., Rizzi, A. & Koditschek, D. (2004). Model-based dynamic self-righting maneuvers for a hexapedal robot, *The International Journal of Robotics Research* 23(9): 903–918.

Schroer, R. T., Boggess, M. J., Bachmann, R. J., Quinn, R. D. & Ritzmann, R. E. (2004). Comparing cockroach and whegs robot body motions, *Proceedings of ICRA 2004 - International Conference on Robotics and Automation*, Las Vegas, Nevada.

Siegwart, R., Lauria, M., Maeusli, P. & Van Winnendael, M. (1998). Design and implementation of an innovative micro-rover, *Proc. of Robotics 98, the 3rd Conference and Exposition on Robotics in Challenging Environments*, Albuquerque, New Mexico.